Biharmonic Spline Wavelets versus Generalized Multi-quadrics for Continuous Surface Representations

Rainer Mautz[1,2], Burkhard Schaffrin[1], Julia Kaschenz[3]

[1] Dept. of Civil and Environ. Eng. and Geodetic Science, Ohio State University, Columbus, Ohio, USA

[2] Institute of Astronomical, Physical and Mathematical Geodesy, Technical University of Berlin, Germany

[3] GeoForschungsZentrum Potsdam, Dept.1: Geodesy and Remote Sensing, Telegrafenberg, Potsdam, Germany

Abstract. In some respect, the continuous representation of surfaces such as the geoid, the topography, or other spatial phenomena, is superior to discrete forms like the TIN (Triangular Irregular Network) or a raster DEM (Digital Elevation Model) as long as these surfaces exhibit a certain degree of local smoothness. In this contribution, we shall concentrate on the special study of biharmonic spline wavelets and of generalized multi-quadrics, with the emphasis on increased efficiency while maintaining the local approximation quality up to the desired resolution.

To support these interpolation techniques a newly developed global search algorithm will be adapted to this problem. It is based on heuristic methods that would allow the user to handle gridded as well as arbitrarily scattered data. The number of coefficients for any surface representation using the global optimization will be extremely small while maintaining a magnitude of deviations that is still acceptable. On the other hand, long computation times have to be taken into account. Concerning the functional model one may face fewer restrictions for its structure when using global methods because no derivatives have to be computed and no approximate values need to be provided.

Some geodetic examples will show the potential of the new techniques, particularly in view of the more classical Fourier analysis.

Keywords. Biharmonic spline wavelets, multi-quadrics, continuous surface representation, global search algorithm

1 Introduction

In geodesy one of the principal research foci is the efficient representation of surfaces. Out of the high number of state-of-the art surface representations only a few can be included in this paper. For a comparison of different methods on a large scale, see Franke (1982). Franke (1987) presents a broad bibliography of 1107 citations related to multivariate approximations. A more recent survey has been carried out by Hubeli and Gross (2000).

All authors mention the difficulty of categorization and the complexity of criteria while trying to rank different methods. Indeed, criteria and their weights depend on the author's emphasis and may include accuracy, timing, storage requirements, ease of implementation, sensitivity to parameters, visual aspects, smoothness / roughness of the surface, ease to compute surface-surface intersections, transitions to different resolutions, possibility of error modeling, behavior at singularities, peaks or cracks, existence of derivatives and gradients. The most important categorization principles differentiate between discrete / continuous, linear / nonlinear and locally / globally supported basis function models.

In the present investigation we shall stick to only four different methods that include the classical Fourier analysis, the multi-quadrics which are well known for their excellent performance, a new family of radial basis functions with local support, and the biharmonic spline wavelets which had been developed for geodetic purposes by Schaffrin et al. (2003). The focus will lie on higher-degree linear versus lower-degree nonlinear models in order to find out how either refinement of the model affects the capability to represent a complex surface.

2 Mathematical Models

"Surface Representations" require the development of continuous surface models from point-sampled data; in effect, it means interpolating and, to some extent, extrapolating point information to cover the continuum. Some mathematical model functions for continuous surface representations are presented.

2.1. a) The 2D-Fourier series:

$$f(x,y)=\sum_{\mu=0}^{\infty}\sum_{\nu=0}^{\infty}A_{\mu\nu}\cos(\mu x)\cos(\nu y) +B_{\mu\nu}\sin(\mu x)\cos(\nu y)+C_{\mu\nu}\cos(\mu x)\sin(\nu y) +D_{\mu\nu}\sin(\mu x)\sin(\nu y) \quad (1)$$

with the frequencies μ, $\nu \in \mathbb{N}_0$ and the amplitudes $A_{\mu\nu}$, $B_{\mu\nu}$, $C_{\mu\nu}$, $D_{\mu\nu} \in \mathbb{R}$. f is a bivariate function from L^2 where the coordinates x and y belong to the interval $[-\pi; +\pi]$. When approximating data $z = f(x, y) + e$, the infinite series is replaced by a summation up to certain integers K_μ and K_ν.

2.1. b) A nonlinear analog to the 2D-Fourier series with flexible frequencies:

$$f(x,y)=\sum_{k=0}^{\infty}A_{\mu_k\nu_k}\cos(\mu_k x)\cos(\nu_k y) +B_{\mu_k\nu_k}\sin(\mu_k x)\cos(\nu_k y)+C_{\mu_k\nu_k}\cos(\mu_k x)\sin(\nu_k y) +D_{\mu_k\nu_k}\sin(\mu_k x)\sin(\nu_k y) \quad (2)$$

The model (2) is no longer harmonic and has been discussed in Kaschenz (2002; 2003) in more detail. It differs from (1) as the frequencies have an extended domain μ_k, $\nu_k \in \mathbb{R}^+$, allowing non-integer ratios between frequencies. However, μ_k and ν_k are unknown parameters, thus making the model (2) *nonlinear*. The series is truncated where the model reaches a predefined precision.

2.2. a) 2-dimensional B-spline wavelets:

$$f(x,y)=\sum_{k_x=1}^{2^{j_{\min}+g}}\sum_{k_y=1}^{2^{j_{\min}+g}}A_{j_{\min},k_x,k_y}\tilde{\phi}_{j_{\min},k_x,k_y}(x,y)+ \sum_{j=j_{\min}}^{J}\sum_{\eta=1}^{3}\sum_{k_x=1}^{2^{j+g}}\sum_{k_y=1}^{2^{j+g}}B_{j,\eta,k_x,k_y}\tilde{\psi}_{j,\eta,k_x,k_y}(x,y) \quad (3)$$

A and B denote the unknown coefficients for the scaling function and the wavelet functions. $\phi(x, y)$ is the 2-D scaling function, $\tilde{\phi}(x, y)$ its dual; $\psi(x, y)$ are the 2-D wavelet functions, and $\tilde{\psi}(x, y)$ their duals. For the reconstruction of the signal only the dual scaling and wavelet functions have to be used, denoted by a tilde. Their polynomial degree is expressed by g. The different levels of detail are denoted by the index j. Wavelet coefficients with a larger j indicate higher detail levels, essentially representing the high-frequency part. The index η denotes the three directional components (horizontal, vertical and diagonal), and the indices k_x, $k_y \in \mathbb{N}_0$ denote the shift of the wavelets to different locations on the (x, y)-patch.

The B-splines on a bounded interval were introduced by Chui and Quak (1992) whereas the related decomposition and reconstruction algorithms were presented in Quak and Weyrich (1994). Via the tensor product at various levels, the 2-D basis functions $\phi(x, y)$ and $\psi_\eta(x, y)$ ($\eta = 1,2,3$) can be generated extremely efficiently. The problem of estimating the coefficients A and B is linear; due to orthogonal subspaces, it is not necessary to solve one big system with linear equations of problem-size, but a sequence of smaller systems. For further details, see Schaffrin et al. (2003).

2.2. b) A nonlinear analog to the 2D B-spline wavelets with flexible dilatation and translation parameters:

$$f(x,y)=\sum_{k=1}^{\infty}B_{j_k,\eta_{lk},x_k,y_k}\psi_{j_k,\eta_{lk},x_k,y_k}(x,y), \quad (4)$$

where $l_k \in \{0, 1, 2, 3\}$. The scaling function ϕ is renamed ψ_0 ($l = 0$) for convenience. To increase flexibility, the dilatation factors $j_k \in \mathbb{R}^+$ are not limited to fixed scales fulfilling 2^j with $j \in \mathbb{N}$. Also the translations x_k and y_k can take any real value in the spatial domain. The directional component of the "pseudowavelets" is kept flexible with the three major directions, allowing $l_k = \{0, 1, 2, 3\}$.

2.3. a) Multiquadrics as radial basis functions with global support:

Out of the large number of radial functions, we pick the well known multiquadrics, introduced by Hardy (1971). Numerical results can be found in Hardy and Hou (1990). Multiquadrics have been a subject of comparison in Franke (1982). Hales and Levesley (2000) introduced a hierarchical approach to determine the coefficients efficiently. Multiquadrics are defined as the upper sheet of a hyperboloid of revolution. Their functional model reads

$$f(x,y)=\sum_{k=1}^{n}A_k\sqrt{r_k^2+c^2} \quad (5)$$

where r_k is given by

$$r_k^2(x,y)=(x-x_k)^2+(y-y_k)^2 \quad (6)$$

as the radial distance between the evaluation point (x, y) and a fixed center position (x_k, y_k) which could be the location of one of the observations. A_k are the unknown parameters and $c \in \mathbb{R}$ is a predefined constant. The estimation of the unknown parameters A_k is a linear problem. An alternative to the multiquadric function is its reciprocal,

$$f(x,y)=\sum_{k=1}^{n}A_k\left(r_k^2+c^2\right)^{-\frac{1}{2}} \quad (7)$$

also known as inverse multiquadric. Figures 1-3 show the radial multiquadric-function for various choices of c, and Figure 4 the inverse multiquadric-function.

2.3. b) Radial basis functions, "multiquadrics" with flexible positions:

$$f(x,y)=\sum_{k=1}^{n} A_k\sqrt{r_k^2+c_k^2}. \qquad (8)$$

The model (8) is similar to (5) except that $x_k \in \mathbb{R}$ and $y_k \in \mathbb{R}$ are unknowns. Also the parameter c is here introduced as an unknown c_k for every $k \in \{1, 2, ..., n\}$. Thus the model is more flexible, but nonlinear and has to be treated as such.

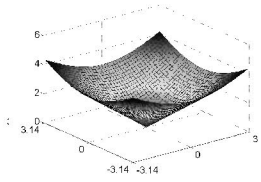

Fig. 1 Multiquadric function with $c = 0$, $A = 1$ and the center in the origin. The surface is a cone.

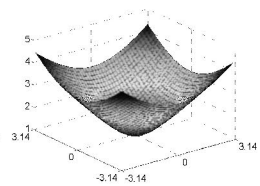

Fig. 2 Multiquadric function with $c = 1$, $A = 1$ and the center in the origin.

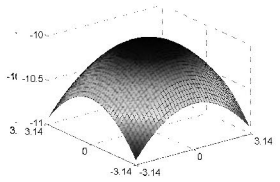

Fig. 3 Negative multiquadric function with $c = 10$, $A = -1$ and the center in the origin.

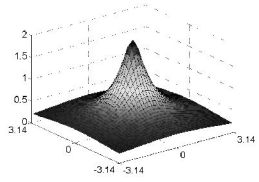

Fig. 4 Inverse multiquadric function with $c = 1$, $A = 0.5$ and the center in the origin.

2.4. a) Radial basis functions with local support, linear model:

When the basis functions differ from zero only within a certain distance from the center point, the represented function depends mainly on the local data. The cut-off can be performed in such a way that there is no discontinuity in the function and in its first derivative. The model (9) with fixed center positions (x_k, y_k) and parameters c_k was considered.

2.4. b) Radial basis functions with local support, nonlinear model:

Again, the nonlinear model

$$f(x,y)=\begin{cases}\sum_{k=1}^{n} A_k\left(\frac{r^2}{c_k^2}-1\right)^2, & r<c_k\\ 0, & r\geq c_k.\end{cases} \qquad (9)$$

is introduced by considering the center positions (x_k, y_k) and the parameters c_k as unknowns for every $k \in \{1, 2,..., n\}$.

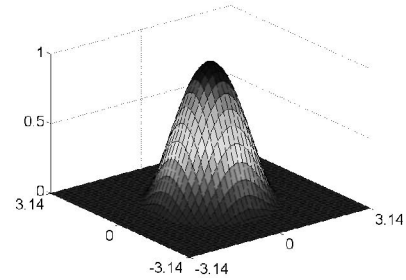

Fig. 5 Radial basis function with local support; Model (9): Polynomial, truncated at $r = c$ with $c = 2.0$, $A = 1$.

3 Solution Techniques for the Linear and Nonlinear Models

Let us work with the linear model

$$\mathbf{y}=\mathbf{A}\xi+\mathbf{e},\ \mathbf{e}\sim\left(0,\sigma_0^2\mathbf{P}^{-1}\right),\ \mathbf{P}:=\mathbf{I}_n,\ \operatorname{rank}(\mathbf{A})=m<n, \qquad (10)$$

where $\mathbf{y}$ is a $n\times 1$ vector of observations (sample of function values), $\mathbf{A}$ is a $n\times m$ matrix of known coefficients, ξ is a $m\times 1$ vector of unknown parameters (typically the "amplitudes" of the basis functions), and $\mathbf{e}$ is the $n\times 1$ random error vector. All observations are assumed to be uncorrelated and of same weight, thus as weight matrix $\mathbf{P}$, the $n\times n$ identity matrix $\mathbf{I}_n$ is chosen. Using BLUUE (Best Linear Uniformly Unbiased Estimator), we obtain the estimated parameters $\hat{\xi}$, the residuals $\tilde{\mathbf{e}}$, and the estimated variance component $\hat{\sigma}_0^2$ with respective variances and covariances:

$$\hat{\xi}=\mathbf{N}^{-1}\mathbf{c}\sim\left(\xi,\sigma_0^2\mathbf{N}^{-1}\right),\quad [\mathbf{N},\mathbf{c}]:=\mathbf{A}^{\mathrm{T}}\mathbf{P}[\mathbf{A},\mathbf{y}],$$

$$\tilde{\mathbf{e}}=\mathbf{y}-\mathbf{A}\hat{\xi}\sim\left(0,\sigma_0^2\left(\mathbf{P}^{-1}-\mathbf{A}\mathbf{N}^{-1}\mathbf{A}^{\mathrm{T}}\right)\right), \qquad (11)$$

$$\hat{\sigma}_0^2=(n-m)^{-1}\left(\mathbf{y}^{\mathrm{T}}\mathbf{P}\mathbf{y}-\mathbf{c}^{\mathrm{T}}\hat{\xi}\right)=\tfrac{\tilde{\mathbf{e}}^{\mathrm{T}}\mathbf{P}\tilde{\mathbf{e}}}{n-m}.\ \hat{\mathbf{D}}\left\{\hat{\sigma}_0^2\right\}=\tfrac{2\hat{\sigma}_0^2}{n-m}.$$

The systems for solving the unknowns in capital letters (e.g., the amplitudes A, B, C, D) are linear if there are no further parameters. In this case, all the position vectors, scaling factors and frequencies are assumed to be known. In fact, they all are set to be constant at certain values, usually equidistant measures that allow efficient algorithms or multi-scaling representations. In the literature, not much effort has been documented to introduce the positions, scaling coefficients and frequencies as unknowns. The resulting models become nonlinear, and the solving techniques require the high computational effort of global optimization methods. Local, nonlinear adjustment strategies like the Gauss-Newton iteration depend on the provision of sufficiently reliable starting values. If they cannot be provided as required, the problem is of global type when applied to the least-squares target function. The common

global techniques such as heuristic methods, interval strategies or genetic algorithms have been sufficiently discussed elsewhere. For instance, global models with unknown frequencies in time series have been studied by Mautz (2001; 2002) while global models for surface data were discussed by Kaschenz (2002; 2003).

4 Comparison of the Models

Due to the high number of potential criteria, a universal ranking of different model functions is impossible. Instead of attempting to weigh different criteria to establish one specific ranking, only the major criteria of the different models will be compared in order to show some of their advantages and drawbacks.

4.0. Premises

Some models necessitate a special data structure for efficient handling. The Fourier series (1) and wavelet analysis (3) use equidistant data points. In addition, multiresolution representations like the wavelet model require a special grid size (e.g. 2^j by 2^j, $j \in \mathbb{N}$). Thus, scattered observations have to be adjusted onto a grid in order to apply these models. The resulting approximation errors from gridding have not been taken into account in this study.

The following comparisons are based on the specific dataset shown in Figure 6.

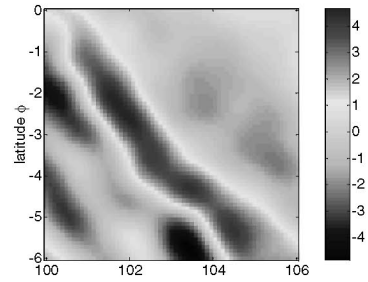

Fig. 6 Height anomalies in [m] from EGM 96, degree and order > 70, between 100° and 106° longitude and 0° to -6° latitude, and sampled onto a 65×65 grid. The range of the data values is [–4.8 m; +4.7 m].

4.1. Adaptation of the model

The residual information is essential for many criteria, which can be expressed by numbers quite well. However, it should not be neglected that the out-

Table 1: Comparison of various surface representation models with a constant number of unknowns; units: [m] or [m^2]

Model	Predetermined coefficients	No. of basis functions	Number of unknowns	C_1: $\max\{\lvert\tilde{e}_j\rvert\}$	C_2: $\sum_{j=1}^{n}\lvert\tilde{e}_j\rvert/n$	C_3: $\tilde{\mathbf{e}}^T\mathbf{P}\tilde{\mathbf{e}}$	C_4: $m_0=\sqrt{\hat{\sigma}_0^2}$
2D-Fourier (linear)	μ, ν	81	289	2.28	0.13	340	0.29
2D-Fourier (nonlinear)	μ_k, $\nu_k \in$ [0; max]	48	288	0.61	0.05	20	0.07
Wavelet, 4 levels	scale of j_0	289	289	0.42	0.05	25	0.08
Wavelet, compression	scale of j_0	289	289 (+ 578)	0.32	0.04	13	0.06
multiquadric (linear)	$c = 0.5°$	289	289	0.34	0.03	8	0.04
multiquadric, flex. pos.	$c = 6°$	96	288	0.80	0.08	46	0.11
multiquadric, c & pos.flex.	$c \in [0°; 1°]$	72	288	0.65	0.08	49	0.11
inv. multiquadric., (linear)	$c = 0.5°$	289	289	0.37	0.04	15	0.06
local radial function	$c = 2°$	289	289	0.68	0.09	70	0.13
loc. rad. func., pos. & c flex.	$c \in [0.05°; 5°]$	72	288	0.23	0.05	14	0.06

Table 2: Number of parameters necessary to achieve a given degree of approximation (in terms of rms)

Model		$m_0=\sqrt{\hat{\sigma}_0^2}$ [m]	$\max\{\lvert\tilde{e}_j\rvert\}$ [m]	No. of basis functions	No. of unknowns	Relative redundancy [%]
2D-Fourier	linear	0.08 m could not be reached. The minimal m_0 = 0.28m (625 unknowns).				
2D-Fourier	nonlinear	0.072	0.61	48	288	93.18
Tensor Wavelet, 4 levels	linear	0.080	0.42	289	289	93.16
Tensor Wavelet, compressed	linear	0.080	0.44	220	220 + (440 integers)	94.80 (89.59)
Multiquadrics (c =0.5°)	linear	0.080	0.51	225	225	94.67
Multiquadrics	nonlinear	0.079	0.48	118	354	91.62
inv. Multiquadrics (c =0.5°)	linear	0.077	0.56	225	225	94.67
local radial function (c = 2°)	linear	0.075	0.46	484	484	88.54
local radial function	nonlinear	0.080	0.29	56	224	94.70

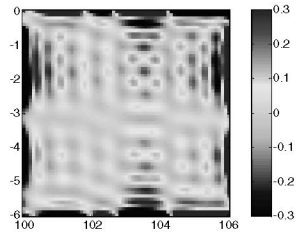

Fig. 7 Residuals of the 2D-Fourier series model (1); 289 basis functions. The unit is [m].

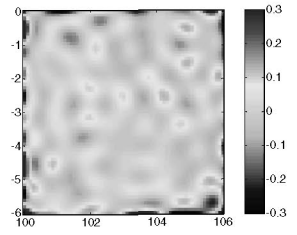

Fig. 8 Residuals of the nonlinear analog to the Fourier series (2); 48 basis functions. The unit is [m].

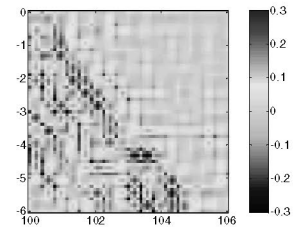

Fig. 9 Residuals of the linear B-Spline Wavelet model (3); 289 basis functions including levels 0 - 4. The Unit is [m].

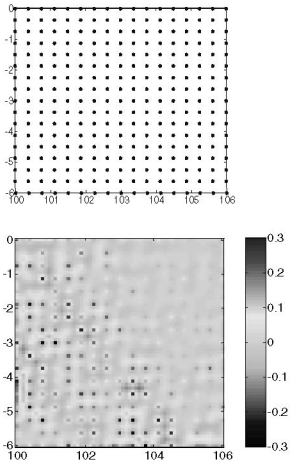

Fig. 10 a-b Linear multiquadric model (5); 289 basis functions with $c = 0.5$. Location of the center points and residuals. The unit is [m].

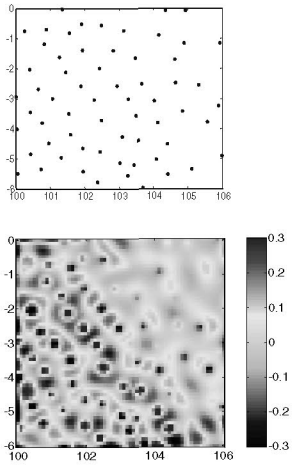

Fig. 11 a-b Nonlinear multiquadric model (8); 72 basis functions with flexible positions and variable parameter c. Location of the center points and residuals. The unit is [m].

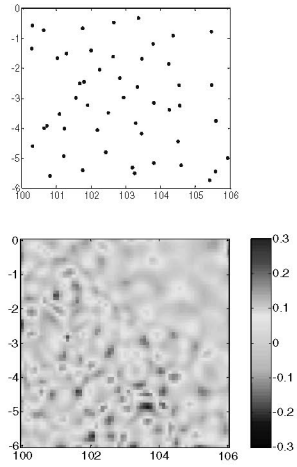

Fig. 12 a-b Nonlinear radial functions with local support (9); 72 basis functions with flexible positions and variable parameter c. Location of the center points and residuals. The unit is [m].

come of such an evaluation strongly depends on the properties of the data. In order to rate the residual information, the following criteria were used:

$$C_1 := \max\left\{\left|\tilde{e}_j\right|, j = 1,2,...,n\right\}, \quad C_2 := \sum_{j=1}^{n}\left|\tilde{e}_j\right| / n,$$

$$C_3 := \tilde{\mathbf{e}}^{\mathrm{T}}\mathbf{P}\tilde{\mathbf{e}}, \quad C_4 := \sqrt{\hat{\sigma}_0^2} = \sqrt{\tilde{\mathbf{e}}^{\mathrm{T}}\mathbf{P}\tilde{\mathbf{e}}/(n-m)}.$$

4.2. Timing

The computational effort depends mainly on the number of observations n and the number of parameters m. In general, linear models involve the solution of a system of $O(m)$ equations. Therefore, it is necessary to set up a system of normal equations $O(n\ m^2)$ and perform an inversion $O(m^3)$. However, there are some exceptions: Orthogonal Fourier basis functions on the continuum - model (1) - would create a diagonal normal matrix, thus the complexity reduces to $O(n\ m)$. The B-spline wavelets - model (3) - are semi-orthogonal and have local support, causing banded matrix structures. Furthermore, the size of the equation systems can be reduced by a factor $m^{-1/2}$. Making use of these properties, the computational effort is $O(n\ m^{1/2})$. The multiquadrics - model (5) - are of complexity $O(n\ m^2)$. If a hierarchical data thinning algorithm is used according to Hales and Levesley (2000), the algorithm may be of linear complexity, but only if the data are spaced equidistantly. However, when the radial basis functions have local support - model (9) - the computational burden decreases drastically. These functions are suitable to handle very large m and n, when globally supported radial functions may not be feasible.

The computing time for nonlinear models is longer than the time for linear models since a global algorithm may require several times to solve a system of linear equations. The computational effort for a nonlinear system will mainly depend on (a) the number of unknown parameters, (b) the possibility to set up a linear system if a fraction of the parameters are kept constant, (c) the global strategy and its implementation, (d) the degree of adaptation

to the problem on hand, (e) the number of local minima of the objective function, (f) the desired precision, and (g) whether the global solution has to be guaranteed. A more detailed discussion can be found in Xu (2002; 2003).

4.3. Smoothness of the surface

The behavior of six different models, namely (1), (2), (3), (5), (8), (9), is visualized in Figures 7-12, for a patch between 100° to 106° longitude and 0° to –6° latitude respectively. All models have 288 (or 289) parameters. As shown in Figure 7 and Table 1, the Fourier series does not represent the data well. In contrast, the nonlinear analog in Figure 8 shows very small residuals in the center.

The wavelet model shows distinct horizontal features. At the center point locations of the multiquadric models, some peaks can be seen.

The locally supported radial basis functions show a smooth surface throughout.

5. Conclusions

In general, linear and local models are computationally efficient. The shortest computation time was obtained for the linear wavelet model.

Using the 2D-Fourier series – model (1) –, one cannot reach the goal of 8 cm rms deviation because, with an increase in the number of parameters, the model improves only very slightly. With the decrease of redundancy the Fourier model reaches the minimal rms of 0.28 cm when $K_\mu = K_\nu = 13$ and the number of parameters is 625. The nonlinear Fourier model has an unexpectedly poor maximum deviation despite a reasonable mean deviation. The linear 2D-Fourier and wavelet models need a data-grid for efficient handling.

The parameter c in the multiquadric model is not very sensitive to the data. Thus c = const. is reasonable. Linear radial basis models need a pre-defined value for c. In order to obtain satisfying results, c has to be optimized prior to their application.

The multiquadric models show peaks, and the wavelet models horizontal and vertical edges in their representations as well as in their residuals.

Nonlinear models generally need a smaller number of basis functions, particularly the locally supported radial functions. Although very time consuming, the smallest number of unknowns was used here to achieve a rms deviation of 8 cm as well as the smallest maximum deviation, but with an enlarged mean deviation when compared with the linear multiquadrics. Note that the nonlinear wavelet model (5) still needs to be studied.

Acknowledgements

R. Mautz acknowledges the partial support of a Feodor-Lynen scholarship of the Alexander-von-Humboldt Foundation (Germany).

References

Chui, C.K., E. Quak (1992): *Wavelets on a bounded interval*; in: Numerical Methods in Approximation Theory, Vol. 9, (D. Braess and L. Schumaker, eds.), Birkhäuser: Basel, Boston, Berlin, pp. 53-77.

Franke, R. (1982): *Scattered data interpolation: Tests of some methods*; Maths. Comp. 38, pp. 181-199.

Franke, R. (1987): *Recent advances in the approximation of surfaces from scattered data*; in: Multivariante Approximation (C.K. Chui, L. Schumaker, and F. Utreras, eds.), Academic Press, New York, pp. 79-98.

Hales S., J. Levesley (2000): *Multi-level approximation to scattered data using inverse multiquadrics*; in: Curve and Surface Fitting: Saint-Malo 1999, (A. Cohen, C. Rabut and L. Schumaker, eds.) Vanderbilt Univ. Press, Nashville/TN, pp. 247-254.

Hardy, R. (1971): *Multiquadric equations of topography and other irregular surfaces*; J. Geophys. Res. 76, pp. 1905-1915.

Hardy, R., Z. Hou (1990): *A new comparative test and a report on the new multiquadric biharmonic method*; AVN-International Edition 7/1990, pp. 4-17.

Hubeli, A., M. Gross (2000): *A survey of surface representations for geometric modeling*; CS Technical Report #335, February 28, 2000, Inst. of Scientific Computing, Swiss Federal Institute of Technology, Zurich, Switzerland.

Kaschenz, J. (2002): *Multidimensional spectral analysis with problem-oriented frequencies* (in German); Dept. of Geodesy and Geoinformation, Tech. Univ. of Berlin, Diploma Thesis.

Kaschenz, J. (2003): *Data modelling using various frequency series* (in German); Z. für Vermessungswesen (ZfV) 128, pp. 260-265.

Mautz, R. (2001): *On the determination of frequencies in time series solving nonlinear adjustment problems;* German Geodetic Comm., C-532, Munich, Germany.

Mautz, R. (2002): *Solving nonlinear adjustment problems by global optimization*; Bollettino di Geodesia e Scienze Affini, Vol. 61, No.2, pp. 123-134, 2002.

Quak, E., N. Weyrich (1994): *Decomposition and reconstruction algorithms for spline wavelets on a bounded interval*; Applied and Comput. Harm. Analysis 1, pp. 217-231.

Schaffrin, B., R. Mautz, C.K. Shum, H. Tseng (2003): *Towards a spherical pseudo-wavelet basis for geodetic applications;* Computer-Aided Civil and Infrastructure Engineering 18, pp. 369-378.

Xu, P. (2002): *A hybrid global optimization method: the one-dimensional case*; Journal of Comp. and Applied Mathematics 147, pp. 301-314.

Xu, P. (2003): *A hybrid global optimization method: The multi-dimensional case*; Journal of Comp. and Applied Mathematics 155, pp. 423-446.